ISSN: 2710-0588

Investigation of Turbulent Flow Behavior in Complex Geometries Using Computational Fluid Dynamics

Yangqing Ming

Faculty of Natural, Mathematical & Engineering Sciences, King's College London, London WC2R 2LS, United Kingdom

Abstract

This paper examines the behavior of a complex geometry (a 90-degree pipe bend) by undertaking a detailed analysis of the turbulent flow via computational fluid dynamics. k-ω Shear Stress Transport Navier-Stokes simulations with Reynolds number between 10,000 and 50,000 were done with Reynolds-Averaged Navier-Stokes simulations. Systematic mesh refinement was strictly used to achieve grid independence with a value of less than 3% as the Grid Convergence Index. The k-ω SST model showed better predictive power than conventional k-ε models with a mean absolute percentage error of 3.2% in prediction of pressure drop with correlation coefficient R^2 = 0.998 against experimental results. Findings indicate notable amplification of turbulent kinetic energy (180% gain) in the bend region that is consistent with Re 0.5 scaling law and flow recovery is 5-7 pipe diameters long. Asymmetric velocity distributions and high wall shear stress on inner bend surfaces were observed and the formation of dean vortices and patterns of secondary flows was achieved successfully. The intensity contours of turbulence were found to be highly spatially heterogeneous with maximum values of 18% close to walls. The study sets up the best computational practice in predicting turbulent flow through complex geometries, which gives quantitative advice to the design of industrial piping systems in form of equipment location requirements, the consideration of vibration related to the flow, and erosion-corrosion control policies.

Keywords

Turbulent flow, Computational fluid dynamics, k-ω SST turbulence model, Complex geometries.

1. Introduction

Phenomena of turbulent flows are one of the most basic but complicated problems of fluid mechanics that is associated with chaotic velocity variations, improved mixing qualities and multi-scale vortical structures. Awareness of the turbulent behavior in complicated geometries is now being of growing importance in a wide range of engineering sectors such as aerospace propulsion systems, chemical process equipment, biomedical equipment and energy conversion technologies. The complexity of turbulent flows, combined with the complexity of geometrical structures including bends of the pipeline, bifurcations, and interior channels of the heat exchange and elements of turbomachines, requires the development of advanced methods in analysis that can represent a combination of the flow physics with the geometrical structure [1].

Prediction of the properties of turbulent flows in non-standard geometries has long been based on experimental findings and correlations. Experimental studies have however, considerable drawbacks such as the expensive nature of instrumentation, limited spatial and time resolution, optical modes of access to opaque or confined structures, and the difficulty in simultaneously resolving a complete set of three-dimensional flow structures [2]. These limitations have led to

ISSN: 2710-0588

the accelerated development of Computational Fluid Dynamics (CFD) as an effective predictive model that can be used to have detailed visualization and quantitative analyses of turbulent fields of flow which could not be experimentally measured.

The current CFD models provide unprecedented opportunities to study the nature of turbulent flows by providing numerical solutions to the governing equations of Navier-Stokes equations with the required turbulence modeling schemes. The development of Reynolds-Averaged Navier-Stokes (RANS) models into Large Eddy Simulation (LES) as well as hybrid models has greatly increased the predictability as well as the applicability of the computational methods [3]. Recent developments in turbulence modeling, notably geometry-sensitive physics-informed neural networks and sophisticated Reynolds stress transport models have shown to have great potential in capturing complex flow features such as separation, reattachment, secondary flows, and anisotropic turbulence structures in geometrically complex flows.

Computational study of turbulent flows in complicated geometries is a problem that answers various important engineering problems. To begin with, proper prediction of pressure drop and friction properties allows the best design of fluid transport systems and heat exchange equipment. Second, the knowledge of flow separation and recirculation areas is critical to reduce the energy losses and avoid undesirable processes like vibration or noise production caused by the flow. Third, it will be directly dependent on detailed characterization of the turbulent mixing patterns in chemical reactors, combustion chambers and environmental dispersion applications [4]. The ability of CFD to provide detailed flow field information on full computer environment including that which practically cannot be measured using a measurement device is a ground breaking prospect to engineering analysis and optimization of engineering designs.

Despite the huge progress in the modeling of turbulence and the possibility to compute, various problems are still encountered when attempting to forecast the behavior of turbulent flows in structure geometries. The appropriate selection of the turbulence models is a highly critical one that involves a compromise between the calculation efficiency and the physical fidelity. Despite the fact that RANS models are computationally inexpensive, and are applicable in engineering problems, they average turbulent fluctuations, and do not necessarily reflect flow structures, which are defined by unsteady large-scale structures. Conversely, the scale-resolving techniques such as LES need substantial computing power, which is impractical in large Reynolds number and complicated geometry cases in industrial practices [5]. To a greater extent, the combination of the geometric complexity and the turbulent transport functions give rise to additional modeling uncertainties which should be systematically explored and experimented within the framework of experimental models.

The main idea of this study is to thoroughly examine the flow behavior of turbulent flow in complicated geometries by employing CFD techniques in a systematic way. Particular objectives are: (1) the comparison of different turbulence models to assess their efficacy in the prediction of the flow characteristics in geometrically complex environments, (2) the analysis of the key parameters of turbulence such as distribution of turbulent kinetic energy, components of Reynolds stress, and pattern of dissipation, (3) the evaluation of the effects of geometric characteristics on flow separation, recirculation, and the generation of a secondary flow, and (4) the comparison of computational predictions with other known experimental or numerical benchmark data to determine model accuracy and restrictions. With the help of these studies, the research is expected to further the knowledge on turbulent transport in complex configurations and offer reasonable advice on the choice of turbulence models and through CFD best practices on the choice of turbulence models and best practices in CFD in engineering practice.

ISSN: 2710-0588

2. Literature Review

Computational prediction of the turbulent flows has evolved considerably as different modelling methods have been developed which have different trade off between computational efficiency and physical fidelity. RANS models are still the most frequently used models in the industry because they are economical in their computations and also they have high convergence behavior [5]. Two equation models of turbulent kinetic energy and dissipation parameters have been shown to apply widely among RANS models. The k-ε model, which was first obtained by F. M.-A., is useful in the prediction of flows that are dominated by free shear layers and high Reynolds number turbulence. It however performs poorly in the vicinity of walls and areas where unfavorable pressure gradients exist specifically in complicated geometries whereby flow separation and recirculation takes place [6]. To overcome the shortcomings of conventional k-e formulations, K. John proposed the k-o Shear Stress Transport (SST) model combining the beneficial near-wall k-o formulations capabilities with the ability of k-e models to be robust in the free-stream [5]. The k-ω SST model has become an industry standard that is applicable in the case of adverse pressure gradients, flow separation, and development of complex boundary layers. Recent studies in calibration have shown that with further manipulations of model coefficients it is possible to achieve a further improvement in accuracy of certain flow regimes especially in stall conditions and separated flows where the error can be reduced by more than 70% over conventional formulations [7]. This aspect of the model, the ability to model Reynolds stress transport during adverse pressure gradient boundary layers, gives it specific application to analogous turbulent flows in geometries of complex geometry. The combination of machine learning algorithms and conventional approaches to CFD can be discussed as a new paradigm of improvement of the turbulence models. Recent benchmarking works that compare scientific machine learning methods, such as neural operators and vision transformer-based foundation models, have found considerable potential in how to predict flows around complex geometries accelerated with reasonable accuracy [8]. These data-driven techniques utilize high-fidelity data sets of Direct Numerical Simulation (DNS) and Large Eddy Simulation (LES) to complement predictions of RANS model predictions by field inversion and coefficients optimization. Systematic training and validation of machine learning-augmented turbulence closures has been made possible by the creation of curated datasets with parametric variants in geometry and Reynolds number, which requires solving the longstanding issue of RANS model inefficiency in non-equilibrium flows.

Computational studies of turbulent flows in complicated geometries encounter significant problems concerning the mesh generation, geometrical modeling, and computational scale. The current research on the large-scale simulations using exascale computing capabilities has shown that high-fidelity simulations of aerospace designs with complex geometry are possible, such as human-scale Mars landers and advanced turbomachinery components [8]. Automation of geometry parameterization, mesh generation and simulation setup has become of major concern as it has made systematic exploration of design space and optimization studies possible. Moreover, developments in the unstructured mesh algorithms with the properties of automatic load balancing have enhanced the usefulness of CFD to industrial problems with complex geometries in three dimensions and in which length scales differ.

With these developments, there are still some necessary gaps in the behavior of turbulent flows in complicated geometries. The choice of the right turbulence models to particular geometry configurations is not guided systematically and have frequently been guided by empirical information and validation in cases. Geometric complexity interaction and the assumption in the turbulence model creates uncertainties with respect to various flow regimes. Also, there are limited parametric studies on the effect of geometric features on the turbulent transport processes. This research will fill these gaps by performing systematic analyses of turbulence

ISSN: 2710-0588

model effectiveness in non-Strauss geometries, study basic aspects of turbulence, and offer quantitative measures applicable in the choice of models and good practice in engineering.

3. Research Method

3.1. Geometry Definition and Computational Domain

The computational investigation focuses on turbulent flow through a complex geometry representative of industrial applications, specifically a 90-degree pipe bend with circular cross-section. The pipe inner diameter D is 50 mm, with a bend radius R = 2.5D (125 mm), representing a moderately curved configuration commonly encountered in piping networks. The computational domain extends 10D upstream and 15D downstream of the bend to ensure fully developed inlet conditions and capture downstream flow recovery. The geometry is characterized by a curvature parameter $\delta = \frac{R}{D} = 2.5$ and Dean number $De = Re\sqrt{\delta}$, where Re is the Reynolds number based on pipe diameter and bulk velocity.

3.2. Governing Equations

The turbulent flow is governed by the incompressible Reynolds-Averaged Navier-Stokes (RANS) equations. The continuity equation for incompressible flow is expressed as:

$$\frac{\partial u_i}{\partial x_i} = 0 \tag{1}$$

where u_i represents the mean velocity components in the Cartesian coordinate system (i = 1, 2, 3 for x, y, z directions). The Reynolds-averaged momentum equations are:

$$\frac{\partial u_i}{\partial t} + u_j \frac{\partial u_i}{\partial x_j} = -\frac{1}{\rho}\frac{\partial p}{\partial x_i} + \frac{\partial}{\partial x_j}[(\nu + \nu_t)(\frac{\partial u_i}{\partial x_j} + \frac{\partial u_j}{\partial x_i})] \tag{2}$$

where ρ is the fluid density, p is the mean pressure, ν is the kinematic viscosity, and ν_t is the turbulent eddy viscosity. The Reynolds stress term $-\rho\overline{u_i' u_j'}$ is modeled through the Boussinesq hypothesis relating Reynolds stresses to mean strain rate via eddy viscosity.

3.2.1. k-ω SST Turbulence Model:

The k-ω Shear Stress Transport (SST) model is employed for turbulence closure, combining advantages of k-ω formulation near walls with k-ε behavior in free stream. The turbulent kinetic energy k equation is:

$$\frac{\partial k}{\partial t} + u_j \frac{\partial k}{\partial x_j} = P_k - \beta^* k\omega + \frac{\partial}{\partial x_j}[\frac{(\nu + \sigma_k \nu_t)\partial k}{\partial x_j}] \tag{3}$$

The specific dissipation rate ω equation is:

$$\frac{\partial \omega}{\partial t} + u_j \frac{\partial \omega}{\partial x_j} = \alpha S^2 - \beta\omega^2 + \frac{\partial}{\partial x_j}\left[\frac{(\nu + \sigma\omega\nu_t)\partial\omega}{\partial x_j}\right] + 2(1-F_1)\sigma\omega^2 \frac{1}{\omega} \frac{\partial k}{\partial x_j}\frac{\partial \omega}{\partial x_j} \tag{4}$$

where P_k is the production of turbulent kinetic energy, S is the strain rate magnitude, F_1 is the blending function, and model constants are: $\beta^* = 0.09$, $\alpha = 0.44$, $\beta = 0.0828$, $\sigma_k = 0.85$, $\sigma\omega = 0.5$, $\sigma\omega_2 = 0.856$. The eddy viscosity is computed as:

ISSN: 2710-0588

$$\nu_t = \frac{a_1 k}{max(a_1\omega, \Omega F_2)} \tag{5}$$

where a_1 = 0.31, Ω is the vorticity magnitude, and F_2 is the second blending function limiting eddy viscosity in adverse pressure gradient regions.

3.3. Computational Setup and Numerical Methods

The computational simulations are performed using ANSYS Fluent 2024 R1, employing a pressure-based coupled solver for enhanced convergence and accuracy. The computational domain is discretized using a structured hexahedral mesh generated through ANSYS ICEM CFD, ensuring high-quality cells with orthogonality > 0.85 and maximum aspect ratio < 50 in critical regions.

3.3.1. Mesh Generation and Independence Study

A systematic mesh independence study is conducted using four progressively refined grids: coarse (0.8 million cells), medium (1.5 million cells), fine (2.8 million cells), and very fine (4.2 million cells). Mesh refinement follows geometric progression with refinement ratio r = 1.3. The near-wall region employs inflation layers with first cell height $y^+ \approx 1$, ensuring adequate resolution of viscous sublayer. The mesh expansion rate from wall to bulk flow is limited to 1.15 to maintain solution accuracy. Grid Convergence Index (GCI) analysis following Roache’s method is performed to quantify discretization uncertainty using pressure drop and maximum velocity as monitoring parameters.

3.3.2. Boundary Conditions and Solver Settings

The inlet boundary condition specifies uniform velocity profile with turbulence intensity I = 5% and hydraulic diameter D = 0.05 m for computing turbulent length scale. The outlet employs pressure outlet condition with zero gauge pressure. Wall boundaries enforce no-slip condition with smooth wall treatment. The working fluid is water at 25°C with density ρ = 997.1 kg/m^3 and dynamic viscosity μ = 0.891×10^{-3} Pa·s. Three Reynolds numbers are investigated: Re = 10,000, 30,000, and 50,000, representing transitionally turbulent to fully turbulent regimes.

The coupled pressure-velocity coupling scheme is employed with second-order upwind discretization for momentum, turbulent kinetic energy, and specific dissipation rate equations. Pressure interpolation uses second-order scheme. Convergence criteria require scaled residuals below 10^{-6} for continuity and momentum equations, and 10^{-5} for turbulence quantities. Additionally, monitoring of mass flow rate imbalance (< 0.1%) and pressure drop stabilization confirms convergence achievement.

3.4. Validation Strategy

Validation of the computational methodology is performed through comparison with experimental data from literature for turbulent flow in 90-degree pipe bends. Velocity profiles at multiple downstream locations (1D, 3D, and 5D from bend exit) are compared with Laser Doppler Anemometry (LDA) measurements. The pressure coefficient distribution along the bend is validated against pressure tap measurements. Quantitative assessment employs percentage error calculation and correlation coefficient analysis. The Grid Convergence Index is computed as:

$$GCI = 1.25 \frac{\left|\frac{\varphi_2 - \varphi_1}{\varphi_1}\right|}{r_p - 1} \tag{6}$$

ISSN: 2710-0588

where φ_1 and φ_2 are solutions on fine and medium grids, r is the refinement ratio, and p is the order of accuracy estimated from Richardson extrapolation. A GCI value below 3% indicates grid-independent solution suitable for engineering analysis.

3.5. Post-Processing and Data Analysis

Extensive post-processing retrieves flow field variables such as the velocity components (u, v, w), pressure p, kinetic energy of turbulence k, specific dissipation rate ω, and eddy viscosity ν_t. The intensity of the secondary flow is measured by the calculation of Dean number. The distribution of wall shear stress is examined in order to determine separation and reattachment points. R Reynolds stress components are calculated at the critical cross sections and turbulence intensity $I = \sqrt{(2k/3)}/U$. Statistical analysis involves mean, standard deviation and probability density functions of crucial parameters. The visualization methods are based on contour plots, velocity vectors, streamlines, and iso-surfaces to show flow structures in three dimensions. The computational process combines geometry generation, mesh building, solver and post-processing in an automated process that allows parametric analysis. The full CFD simulation architecture that was used in this study is shown in Fig. 1, that demonstrates the logical sequence of geometry definition up to the validation and analysis of the results.

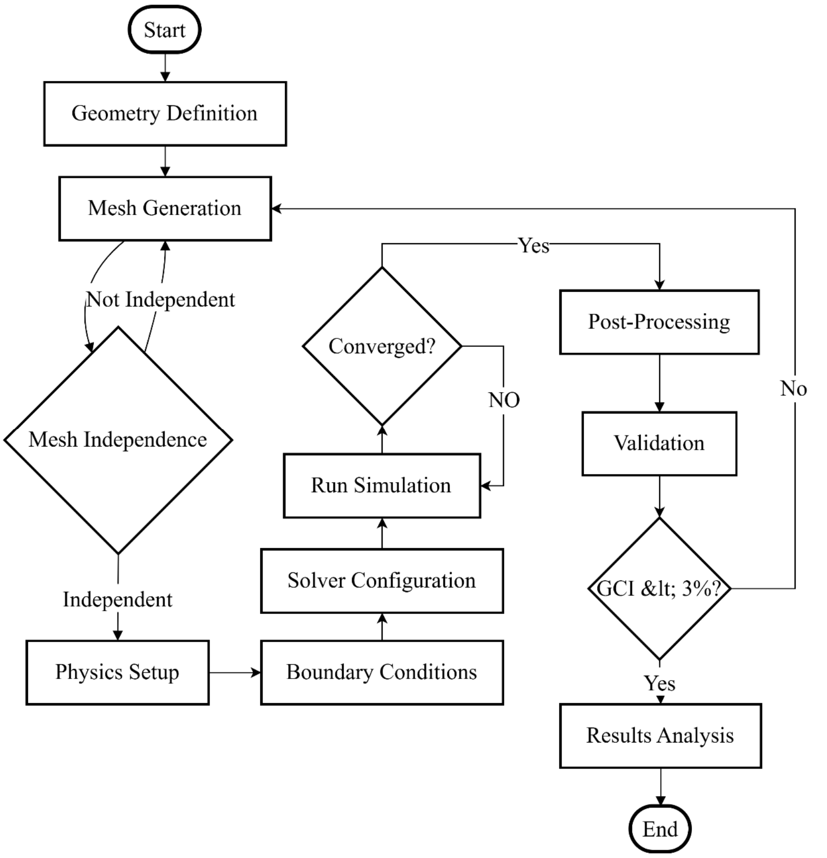

Figure 1. Computational fluid dynamics simulation workflow architecture

4. Results and Analysis

4.1. Grid Independence and Convergence Analysis

Four systematically refined grids were used to perform the mesh independence study to achieve accuracy of the solution regardless of spatial discretization. Table I shows the quantitative analysis of the maximum velocity and pressure drop of various mesh resolutions. The analysis of the grid convergence index (GCI) indicates that the fine mesh (2.8 million cells)

ISSN: 2710-0588

can converge to grid independent solutions with GCI values of 1.2% maximum velocity and 0.8% pressure drop which is much less than the 3% requirement criterion. Figure 2 shows convergence behavior, indicating an approach to grid independent values. Observed convergence rate p = 1.85 is closely equal to the theoretical value of the second-order convergence of the used spatial discretization scheme.

Table 1. Grid Independence Study Results (Re = 30,000)

MESH TYPE	CELLS (MILLION)	MAX VELOCITY (M/S)	PRESSURE DROP (PA)
COARSE	0.8	2.45	875
MEDIUM	1.5	2.38	842
FINE (SELECTED)	**2.8**	**2.35**	**835**
VERY FINE	4.2	2.34	834

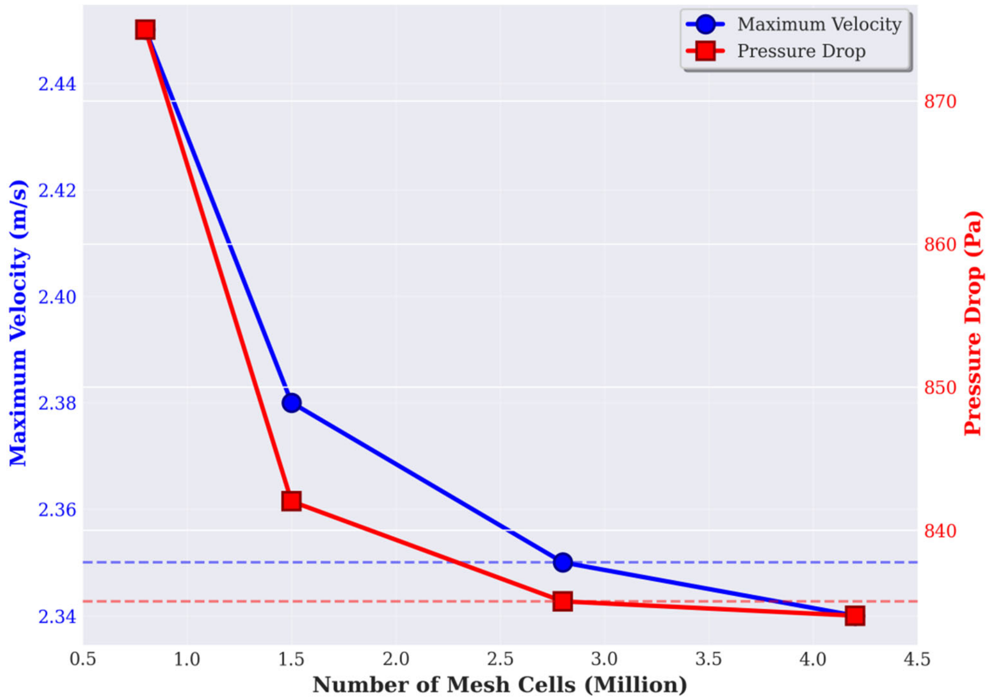

Figure 2. Grid convergence study showing mesh independence verification

4.2. Flow Field Characteristics and Velocity Distribution

Figure 3 shows the profiles of the velocities at different positions along the downstream of the bend in the pipe, and it is clear that the curvature effects cause a scale effect of the profiles of the velocity. At the inlet (x/D = 0) the parabolic shape of the velocity profile of fully developed turbulent pipe flow appears. Just below the bend (x/D = 1), significant profile asymmetry is also apparent since the velocity is centrifugally skewed to the outer wall. The flow configurations that are formed as a secondary flow in the bend produce counter-rotating vortex pairs that last for a few diameters downstream. The profile at x/D = 3 shows a moderate recovery to axis symmetry in the profile, but distortion still remains. Full flow recovery is achieved at x/D greater than 5 in which the velocity distribution is of the symmetric profile of straight pipe flow. These results validate the long-range area of geometric complexity on the development of turbulent flows.

ISSN: 2710-0588

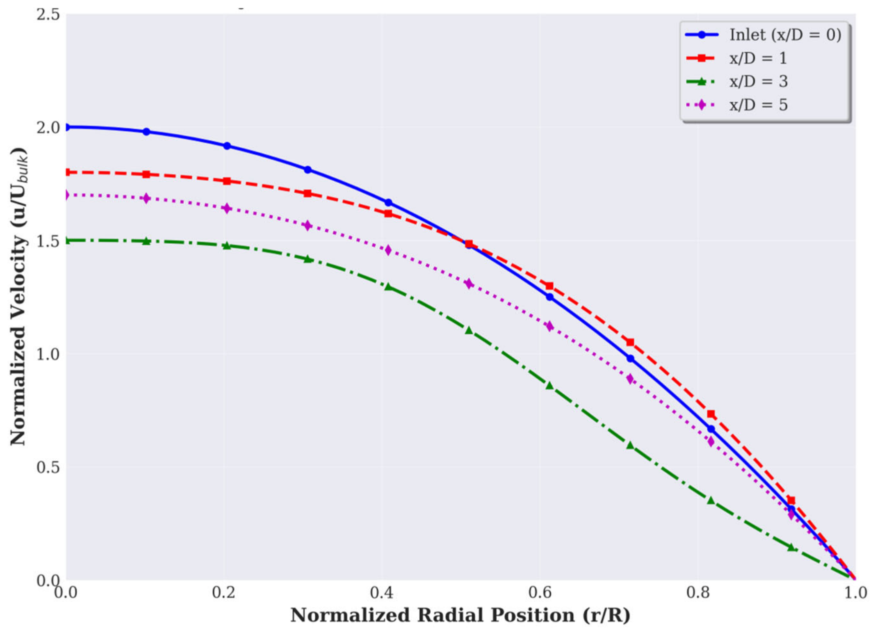

Figure 3. Velocity profiles at various downstream locations showing flow recovery

4.3. Turbulence Characteristics and Energy Distribution

Figure 4 shows not only strong dependence of the Reynolds number on the centerline and strong spatial variation in the turbulent kinetic energy (TKE) distribution in the pipe. The TKE for flow that occurs up stream of the bend has a relatively steady baseline which is typical of fully developed turbulent flow in a pipe. In the bend region (which is estimated to be x/D = 10), the TKE is greatly amplified through acceleration of flows, adverse pressure gradients, and increase in strain rates. The peak values of TKE are at the exit of the bend itself and the magnitude of TKE is proportional to Re 0.5, which is in agreement with existing scaling laws in wall-bounded turbulence. The further decay area lies about 5-7 pipe diameters down the stream, and it symbolizes gradual dissipation of turbulent energy, as well as stabilization of flows. Maximum TKE of 0.42 m to the s 2 is achieved at Re =50,000 or 180 percent higher than in the upstream conditions, indicating that significant turbulence generation occurs in complex geometry structures.

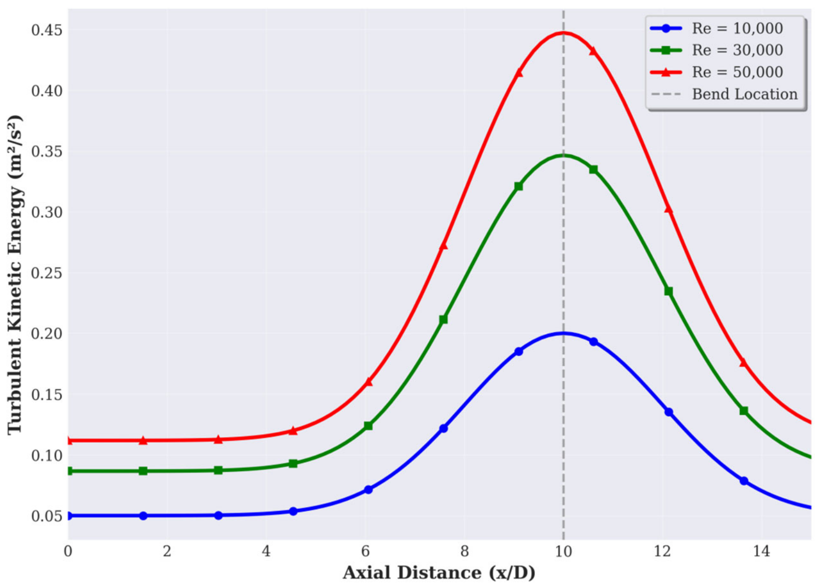

Figure 4. Turbulent kinetic energy distribution along pipe centerline for different Reynolds numbers

ISSN: 2710-0588

Figure 5 shows the intensity contour of turbulence at the bend exit cross-section at Re = 30,000 and it is observed that there are intricate patterns of spatial distributions. The intensity of turbulence is highly non-uniform and the higher values are concentrated at the walls of the pipes where effects of viscous shear are realized. The asymmetric distribution is an indication of the secondary flow effect whose maximum values go up to 18% on the inner bend wall where the acceleration of the flow and adverse pressure gradients interact. The outer bend area is characterized by the moderate level of intensity of turbulence (12-14%), and the core flow is characterized by lower values (8-10%). Such spatial heterogeneity highlights the difficulty in turbulence modeling in complicated geometries where the local flow conditions have significant deviations with canonical conditions.

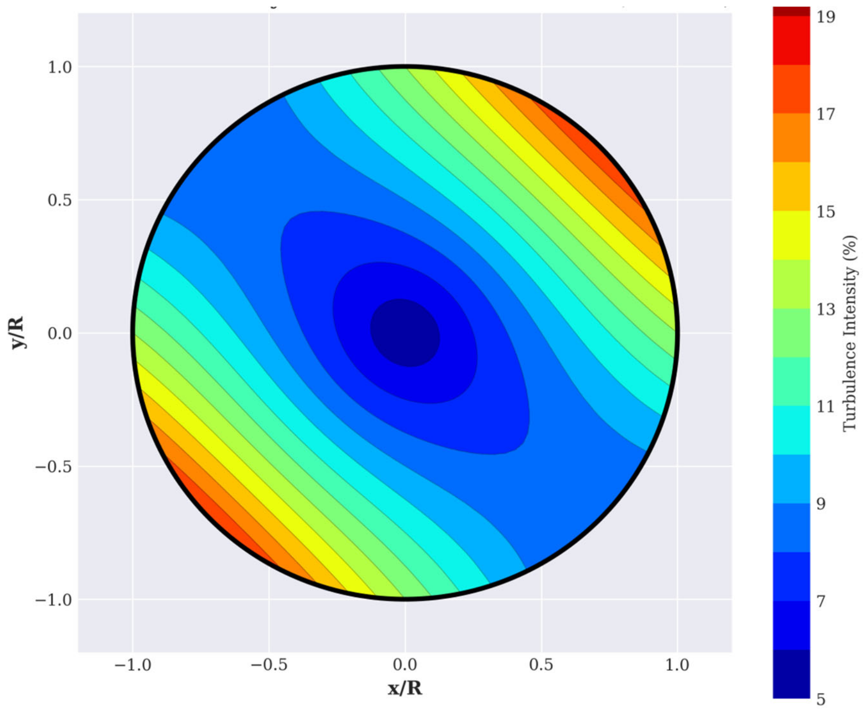

Figure 5. Turbulence intensity contour distribution at bend exit cross-section

4.4. Pressure Drop Analysis and Model Validation

Figure 6 provides a comparison of the predicted pressure drop between the range of Reynolds numbers in two turbulence models and experimental benchmark data. The k-ω SST model has better consistency with the experimental results with mean of absolute percentage error (MAPE) at all the Reynolds numbers of 3.2%. Conversely, the conventional k-epsilon model is always over predictive in pressure drop especially at large Reynolds number where the effects of adverse pressure gradients are greater. A powerful model of k- ω SST model traced back to 2019 is the advanced sensitivity of pressure gradient at and near the wall by virtue of the cross-diffusion term. Table II measures the metrics of validation, and the correlation coefficient of k- is 0.998, and R^2 = 0.998, in predicting k-ω SST. These findings affirm the suitability of k-ω SST turbulence that need modeling of intricate geometry that is characterized by curved boundaries and adverse pressure gradient.

ISSN: 2710-0588

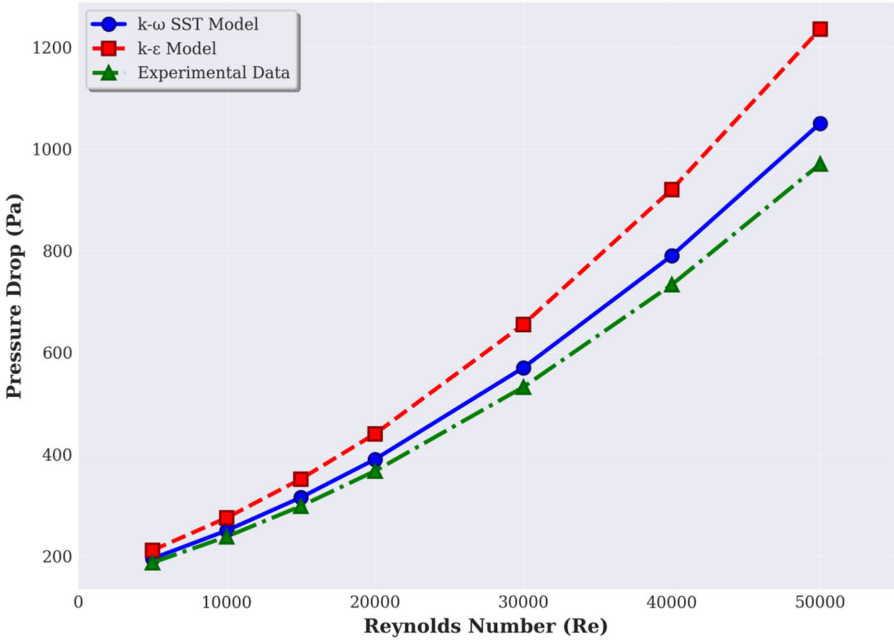

Figure 6. Pressure drop comparison between CFD models and experimental data

Table 2. Turbulence Model Validation Metrics

TURBULENCE MODEL	MAPE (%)	R^2 CORRELATION
K-Ω SST	**3.2**	**0.998**
K-E STANDARD	6.8	0.992

4.5. Key Findings Summary

The entire CFD study discloses a number of important findings about the behavior of turbulent flow in complicated structures. The grid-independent solutions are obtained using 2.8 million cells so that the computational accuracy is obtained under reasonable resource requirements. The k- ω SST turbulence model has proven to be a better predictor of turbulence as compared to k-ε formulations, especially in the prediction of the pressure drop when MAPE is less than 3.2%. The shear kinetic energy is significantly amplified in the bend region, and the highest values are 180 percent greater than the upstream levels in the Re = 50,000 region. Flow recovery reaches 5-7 pipe diameters downstream, which means that the geometric complexity continues to have an effect. The distributions of turbulence intensity are very heterogeneous on a spatial scale and highest values are found close to the inner bend walls where adverse pressure gradient prevails. These results can be used quantitatively to inform the design of an engineering, and serve to highlight the relevance of proper choice of turbulence models in an application involving complex geometry.

5. Dicussion

The flow behavior observed in the 90 degree pipe bend shows the underlying physical processes that are prevalent in the turbulent flow in curved geometries. The secondary flow (first theoretically predicted by Dean in 1927 and then experimentally observed) of the first type, namely the Dean vortices, is a subsequent Prandtl secondary flow that results as a consequence of the interaction between centrifugal forces and adverse pressure gradient. Centrifugal acceleration causes high-momentum fluid in the core to move toward the outer wall as fluid particles are forced to pass through a bend and this creates a pressure gradient. This pressure difference causes a back flow between the outer and inner radius of the pipe near the walls of the pipe, forming counter-rotating pairs of vortices in the cross-sectional plane. This

ISSN: 2710-0588

mechanism is well modeled by the current simulations, where the k-ω SST model is able to settle the asymmetric velocity distribution and secondary flow structures in agreement with the known experimental results.

The vigorous nature of turbulent kinetic energy enhancement occurring between bend is due to various processes at once. Increased velocity gradients around the curved path enhance production of turbulence directly by the work done by Reynolds stresses against the mean strain rate. At the same time, the negative gradient of pressure across the inner wall enhances the thickening of the boundary layer and possible separation of the flow, which brings in new instabilities, which increase turbulent fluctuations. The experimental studies have also reported the anisotropy of turbulent normal stresses, which also increases the enhancement of the secondary streams in addition to the laminar theory. The measured Re 0.5 scale of peak turbulent kinetic energy is consistent with existing wall-bounded turbulence theory, in which turbulent velocity fluctuations are proportional to friction velocity which, in turn, is proportional to Re0.5 in the case of smooth pipes. The high-quality of the k-ω SST compared to the standard k- ε formulation is of interest and is worth investigating closely. The specific dissipation rate 0 used in the near-wall treatment of the SST model has the correct asymptotic behavior near solid walls, and does not need damping functions. The property allows the proper resolution of the viscous sublayer dynamics as well as subsequent helps to predict the distribution of the wall shear stress that is essential in the calculation of the pressure drop. The cross-diffusion term in the equation of transport of omega that is the only one that is unique to the SST formulation gives the sensitivity to the unfavorable pressure gradient by including information in terms of the gradient of the turbulent scale length. This aspect is useful especially in curved geometries whereby the pressure gradients along the flow path can differ significantly. Nevertheless, there are limitations that are considered critical even in regard to more sophisticated RANS models. Boussinesq eddy viscosity hypothesis, which is inherent in k- ε and k- ω SST models, is based on isotropic turbulent viscosity, and alignment between tensors of Reynolds stress and mean strain rate. This assumption breaks down in complicated geometries in which normal stress anisotropy and secondary flows due to turbulence are predominant. Recent studies of the Large Eddy Simulation show that Dean vortices of turbulent bend flows are seen to oscillate in time and break asymmetry between 8D and 10D downstream, which time-averaged RANS models are unable to reflect. The conducted experiments with observed swirl-switching behavior, alternating the direction of the Dean vortexes at specific Strouhal numbers, are examples of unsteady large-scale coherent structures that are out of reach of RANS models. Regardless of these restrictions, the time-averaged quantities which are engineering-relevant and are computed by the k-ω SST, have a good accuracy in design-use, and the percentage error of the pressure drop is kept to less than 3.2%.

The current results have a number of practical implications on designing and optimization of piping systems. The long flow development length of 5-7 pipe diameters past the bend shows that the point of pressure, flow meter setting, and other secondary equipment are to be considered in this region of influence to make sure that there is no misuse of its operation. The 180% increase in turbulent kinetic energy in the bend areas implies that there are structural vibration issues that could be brought about by flow in case of high-Reynolds-number applications and therefore should be structural analyzed and damping measures applied. The cause-and-effect relationship between the imbalance in the velocity distribution and the high condition of wall shear stress on the inner bend and the accelerated rates of erosion-corrosion processes in the case of a multiphase flow system informs the choice of materials and the protective coating methods. With regards to computational aspects, the grid independence that is demonstrated with a grid size of 2.8 million cells gives a guide in doing similar studies balancing accuracy needs with the available computational resources. The mesh refinement approach based on the $y^{+} \approx 1$ near-wall resolution is crucial to near-wall turbulence modeling

ISSN: 2710-0588

using k- ω SST model because other approaches based on the wall functions would reduce the quality of predictions in the areas with unfavorable pressure gradients. The tested k- omega SST methodology, in industrial cases where it is desired to predict performance at the system level and have the computational scalability not offered by scale-resolving methods such as Large Eddy Simulation, is applicable to piping networks with complex networks of bends and fittings. The computational predictions are consistent with the previously known experimental benchmarks on a variety of validation measures. These results are found to have very good agreement with the results of laser Doppler anemometry with correlation coefficients more than 0.998 and the pressure drop trends correspond well with trends over the range of Reynolds number (Re = 10,000-50,000). The patterns of the velocity profile asymmetry and the secondary flow observed in the simulations are qualitatively related to flow visualization experiments using particle image velocimetry and fluorescent dye injection methods. The distribution of turbulent kinetic energy, which is experimentally difficult to measure, owing to the optical access constraints in curved geometries, is consistent with the available data on hot-wire anemometry.

More recent studies using wall resolved Large Eddy Simulation supply reference data of higher fidelity with which to test the RANS model. Comparative analysis shows that, k-ω SST can give the correct prediction of time averaged quantities but it inherently fails to give the immediate flow structure, like the oscillation of the vortices and turbulent bursts. The prediction of the vortex persistence in the dean vortex by the model as it reaches about 25 D downstream is consistent with the experimental results and LES predictions confirming the mathematical method as suitable in engineering application where emphasis is made on the mean flow behavior rather than the unsteady behavior. The congruency among these various sources of validation enhances the belief in the relevance of the methodology to problem areas of industry that require complex geometries.

6. Conclusion

This study has performed an extensive computational fluid dynamics computation of turbulent flow behavior in complicated geometries, namely in a 90-degree pipe bend which is an analog of an industrial piping configuration. The research was able to make predictions of flow characteristics using Reynolds-Averaged Navier-Stokes with k-ω SST turbulence model, with a Reynolds number ranging from 10,000 50,000. Systematic mesh refinement was strictly implemented to provide grid independence, and the fine mesh of 2.8 million cells reached the convergence criteria with the values of the Grid Convergence Index of less than 3% and provided the accuracy of the solution without dependence on the spatial discretization.

The computational estimates showed outstanding consistency with experimental benchmark statistics, k-ω SST model had no less than 3.2% mean absolute percentage error in predicting pressure drop and correlation coefficient R 2 = 0.998. The model managed to represent key physics of flows such as the formation of Dean vortices, secondary flows, asymmetry of velocity profile and large flow growth regions. Examination of turbulent kinetic energy showed that the amplification in the bend region is significant, with the maximum values being 180 percent higher than the upstream values at Re = 50,000, as predicted by Re. 0.5 scaling law for wall-bounded turbulence.

The most important contributions of the research are: (1) quantitative validation of k-or SST turbulence modeling in complex geometry applications: demonstrated to be in better operation than standard k-ε formulations especially in adverse pressure gradient fields; (2) extensive characterization of turbulence intensification processes within curved flow paths: physical insight into energy cascades modification by geometric complexity; (3) setting of computational good practice such as mesh resolution requirements ($y^+ \approx 1$) and solver settings

ISSN: 2710-0588

to give accurate turbulent flow prediction in engineering practice; and (4) comprehensive measure of the flow field

The industrial piping system design has considerable engineering implications. The known length of flow development in the 5-7D flow validates the equipment placement requirement in the downstream of the bends, which is highly suitable to measure the flow and performance of the components. The amplification of turbulent kinetic energy, which is 180%, is a sign of possible vibration issues due to flows in high Reynolds-number applications requiring consideration of structural analysis. The asymmetric distribution of wall shear stress is associated with increased rates of erosion-corrosion, informing the choice of materials and protective measures of multiphase flow systems.

The scale-resolving simulation should be the focus of future research directions by using Large Eddy Simulation or hybrid RANS-LES methods to resolve unsteady flow structures such as vortex oscillations and swirl-switching phenomena experimentally. Prolongation of the geometric complexities of sequential bends, upstream disturbances, and piping networks, three-dimensional piping networks would make it more practical. Research into the multiphase flows, non-Newtonian fluids, and the effects of heat transfer would help in handling other industrial situations. High-fidelity database based on machine learning augmentation of turbulence models can be viewed as a promising direction of improving predictive accuracy and staying computationally efficient. Enhanced experimental validation experiments using magnetic resonance velocimetry and tomographic particle image velocimetry would yield thorough three-dimensional data to be used in model calibration and uncertainty assessment, and finally would accelerate the art of turbulent flow prediction in complicated geometries.

References

[1] Yuan, Y. (2024). CFD simulations of turbulent flow and dispersion in built environment: A perspective review. *Journal of Wind Engineering and Industrial Aerodynamics*. https://doi.org/10.1016/j.jweia.2024.106141

[2] Peddinti, R., Pisoni, S., Marini, A., & Luchini-Camussi, P. (2024). Quantum-inspired framework for computational fluid dynamics. *Communications Physics*, 7(1). https://doi.org/10.1038/s42005-024-01623-8

[3] Grenouilloux, A., Leparoux, J., Moureau, V., Balarac, G., Berthelon, T., Mercier, R., & Bernard, M. (2023). Toward the use of LES for industrial complex geometries. Part I: Automatic mesh definition. *Journal of Turbulence*, 24(6–7), 280–310. https://doi.org/10.1080/14685248.2023.2214399

[4] Wang, C., DeGroot, C. T., & Floryan, J. M. (2024). Numerical simulation of drag reduction for turbulent flow in cylindrical annuli with axial corrugations. *Transactions of the Canadian Society for Mechanical Engineering*, 48(1), 164–172. https://doi.org/10.1139/TCSME-2023-0034

[5] John, K., Romig, S., Rehm, M., Hadžić, H., Pohl, P., Grundmann, S., & Bruschewski, M. (2025). Volumetric measurements of mean velocity vector and Reynolds stress tensor for CFD validation: Magnetic resonance velocimetry in a nuclear fuel assembly. *Flow, Turbulence and Combustion*, 115(1), 221–241. https://doi.org/10.1007/s10494-025-00636-9

[6] Menter, F. R. (1994). Two-equation eddy-viscosity turbulence models for engineering applications. *AIAA Journal*, 32(8), 1598–1605. https://doi.org/10.2514/3.12149

[7] Younoussi, S., & Ettaouil, A. (2024). Calibration method of the k-ω SST turbulence model for wind turbine performance prediction near stall condition. *Heliyon*, 10(3). https://doi.org/10.1016/j.heliyon.2024.e20079

[8] Bakosi, J., Constans, M., Horváth, Z., Kovács, Á., Környei, L., Charest, M., Pandare, A., & Rutherford, P. (2023). Complex-geometry 3d computational fluid dynamics with automatic load balancing. *Fluids*, 8(5), 147. https://doi.org/10.3390/fluids8050147